PARAMETRIC STUDY OF A CONFINED STAGNATION METHANE-AIR DIFFUSION FLAME

Antonio Pereira Roseira Júnior
Missile and Rocket Section/ Military Division - Centro Tecnológico do Exército
Av. das Americas, 28705 - Rio de Janeiro – RJ - 23020-470 - Brazil
aroseira@ctex.eb.br

Albino José Kalab Leiroz
Department of Mechanical Engineering, POLI/ COPPE - Universidade Federal do Rio de Janeiro
Cx. Postal 68503 - Rio de Janeiro – RJ - 21945-970 - Brazil
leiroz@ufrj.br

Abstract. *This work presents the numerical investigation of the non-premixed methane-air flame in a counterflow slot burners configuration, confined by solid walls. The temporal evolution of the flow, temperature and chemical species concentration fields are studied. The Finite-Difference Method is employed on the mass, momentum, energy and chemical species conservation equations, which are written in a Cartesian system of coordinates and discretized using the BTCS (Backward in Time Forward in Space) scheme. The Vorticity-Stream function formulation is used to solve the Navier-Stokes equations while the Shvab-Zel'dovich formulation solves the energy and chemical species ones. An iterative numerical technique, based on successive under-relaxation and local error control, is applied to solve the resulting system of algebraic equations. A parametric study is conducted for different inflow velocities ratio, and the results show the effects on the flame shape characteristics, subject to the presence of recirculation zones.*

Keywords*: diffusion flame, counterflow, vorticity-stream function, Shvab-Zel'dovich formulation.*

1. Introduction

Advances in computational algorithms and computer capabilities have provided new and extremely powerful tools for the investigation of chemically reacting systems that were computationally infeasible only a few years ago. Diffusion flames are one such example. The interaction of heat and mass transfer with chemical reactions in commercial burners, gas turbines, and ramjets, these flames are important examples of application where diffusion flames are found (Douglas, 1996).

The counterflow flame is a commonly used geometry for experimental combustion and chemical kinetic modeling studies of non-premixed combustion. Studies on interaction of laminar vortices generated from either the fuel side or the oxidizer side (Santoro *et al*, 1999), on flame-extinction phenomena (Pellet *et al*, 1998, Daou and Liñán, 1999), on the dilution limits of diffusion flames are examples of the usage of the counterflow configuration. The counterflow configuration is also found in studies on the overall reaction rates for fuel-oxidant combinations, the effectiveness of inhibitors (Tsuji, 1982), the transient phenomena during diffusion/edge flame transition (Frouzakis *et al*, 2002) and the burning of multicomponent fuels in a diffusion flame (Fachini, 2001, 2004).

Since the flame structure is quasi-one-dimensional and more computationally tractable than inherently multidimensional flame geometries (Williams, 2001), detailed chemical kinetic modeling codes for counterflow flames have come into widespread use.

In the present work, a parametric study is proposed to investigate the influence of recirculation zones on the flame shape in the laminar regime, considering variations on the oxidizer inlet velocity, represented by a velocitiy-ratio. Analyzing the stream function distribution field it is possible to locate recirculation zones by the flow pattern lines.

2. Physical and Mathematical Model

The physical model involves the combustion of separate streams of fuel and oxidizer in gas-phase in a counterflow slot burner configuration. The configuration is commonly used in numerical and analytical studies since results are easily verified experimentally due to the easy access in the flame region (Fachini, 2001). The thermo-physical properties are assumed constant. In order to solve the Navier-Stokes equations, the Vorticity-Stream function formulation is employed, eliminating the pressure as a dependent variable from the momentum conservation equations and reducing the number of equations to be solved simultaneously. The continuity equation is identically satisfied by the stream function definition. The Vorticity-Stream function formulation presents a difficulty in the specification of vorticity boundary conditions. It is necessary to specify vorticity values along the solid boundaries in terms of the stream function, which requires the discretization using second order derivatives. Along the symmetry plane, zero-vorticity boundary condition is applied.

The Simple Chemical Reaction System hypothesis is employed and the values of diffusivities of mass and energy are considered equal for each species. The mathematical model is based on the mass, momentum and Shvab-Zel'dovich potential conservation equations as described by Anderson *et al* (1984) and Kuo (1986).

3. Geometry

The geometry adopted to represent the physical half-domain is described in a Cartesian system of coordinates by four boundaries (Fig.1). The left boundary represents the flow field symmetry plane and the nozzle separation width (L^*), the right boundary is the outflow region, as well as the truncation position in the horizontal direction. The top and bottom boundaries (P^*) include the fuel and oxidizer nozzles widths, respectively, D_F^* and D_O^*, and the solid walls, which are considered adiabatic and nonreactive (Tomboulides *et al*, 1997, Santoro *et al*, 1999, Frouzakis *et al*, 2002, Chaniotis *et al*, 2003).

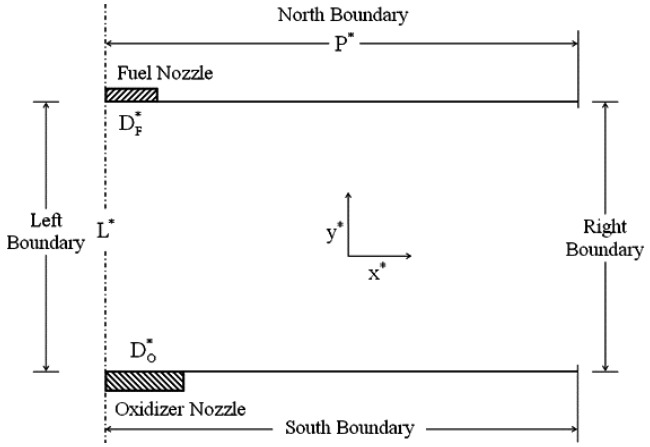

Figure 1. Geometry adopted representing a half-domain.

Santoro *et al* (1999) reported methane-air edge flames stabilized on an axisymmetric counterflow burner with two parallel circular plates attached to the nozzle exists to confine the flow in the radial direction, and minimize entrainment while providing well-defined boundary conditions.

4. Governing Equations, Initial and Boundary Conditions

The definitions of the dimensionless groups employed in the following equations are given in Eqs. 1.a-j.

$$x = \frac{x^*}{D_F^*} \quad ; \quad y = \frac{y^*}{D_F^*} \quad ; \quad L = \frac{L^*}{D_F^*} \quad ; \quad P = \frac{P^*}{D_F^*} \quad ; \quad u = \frac{u^*}{\left|U_F^*\right|} \quad ; \quad v = \frac{v^*}{\left|U_F^*\right|}$$
$$\omega = \frac{\omega^* D_F^*}{\left|U_F^*\right|} \quad ; \quad \psi = \frac{\psi^*}{\left|U_F^*\right|.D_F^*} \quad ; \quad t = \frac{t^* \left|U_F^*\right|}{D_F^*} \quad ; \quad \theta = \frac{T^* - T_F}{T_O - T_F} \tag{1.a-j}$$

where U_F^* is the fuel maximum velocity along the fuel nozzle, T_F and T_O represent the fuel and oxidizer inflow temperatures, respectivelly.

4.1. Description of the Flow Field

The hydrodynamic system is described by the Navies-Stokes equations: mass and momentum conservation equations. However, by introducing the Vorticity-Stream function formulation, we can manipulate the momentum equations and use the definition of vorticity as

$$\omega = \frac{\partial v}{\partial x} - \frac{\partial u}{\partial y} \tag{2}$$

which results in a Vorticity Transport equation

$$\frac{\partial \omega}{\partial t} + u\frac{\partial \omega}{\partial x} + v\frac{\partial \omega}{\partial y} = \frac{1}{Re}\left(\frac{\partial^2 \omega}{\partial x^2} + \frac{\partial^2 \omega}{\partial y^2}\right) \tag{3}$$

The Reynolds number is defined based on the fuel nozzle

$$\mathrm{Re} = \frac{\left|U_F^*\right|.D_F^*}{\upsilon} \quad ; \tag{4}$$

where υ represents the fuel kinematic viscosity. Stream function $\psi(x,y)$ is defined, using the velocity components in order to satisfy the continuity equation, as

$$u = \frac{\partial \psi}{\partial y} \quad ; \quad v = -\frac{\partial \psi}{\partial x} \tag{5.a-b}$$

Replacing the velocity components Eqs.(5.a-b) in Eq.(2), we obtain the Poisson's equation for the stream function.

$$-\omega = \frac{\partial^2 \psi}{\partial x^2} + \frac{\partial^2 \psi}{\partial y^2} \tag{6}$$

The parabolic velocity profile was used to represent the inflow velocity conditions at the nozzles and at the outflow boundaries. Therefore, the velocities boundary conditions must be expressed in terms of stream function, as:

$$\begin{aligned}
&\psi = 0 \quad ; \quad x = 0 \ , \ 0 < y < \frac{1}{R_{DL}} \\
&\psi(x) = \frac{3x}{2}\left(1 - \frac{x^2}{3}\right) \quad ; \quad 0 \le x \le 1 \ , \ y = \frac{1}{R_{DL}} \\
&\psi = 1 \quad ; \quad 1 < x \le R_H \ , \ y = \frac{1}{R_{DL}} \\
&\psi(y) = y^2 R_{DL}{}^2 \left(1 + R_V.R_B\right)\left(3 - 2\,y\,R_{DL}\right) - R_V.R_B \quad ; \quad x = R_H \ , \ 0 < y < \frac{1}{R_{DL}} \\
&\psi(x) = -\frac{3x R_V}{2}\left[1 - \frac{1}{3}\left(\frac{x}{R_B}\right)^2\right] \quad ; \quad 0 \le x \le R_B \ , \ y = 0 \\
&\psi = -R_V.R_B \quad ; \quad R_B < x \le R_H \ , \ y = 0
\end{aligned} \tag{7.a-f}$$

The following dimensionless ratios represent, respectively, the fuel nozzle width-separation distance, the horizontal aspect, inflow peak velocities, and nozzle width ratios.

$$R_{DL} = \frac{D_F^*}{L^*}, \quad R_H = \frac{P^*}{D_F^*}, \quad R_V = \frac{U_O^*}{\left|U_F^*\right|}, \quad R_B = \frac{D_O^*}{D_F^*} \tag{8}$$

4.2. Thermo-Chemical Model

The thermo-chemistry system is described by the energy and chemical species equations:

$$\frac{\partial \theta}{\partial t} + u\frac{\partial \theta}{\partial x} + v\frac{\partial \theta}{\partial y} = \frac{1}{Pe}\left(\frac{\partial^2 \theta}{\partial x^2} + \frac{\partial^2 \theta}{\partial y^2}\right) + \frac{\dot{\omega}_F^* \Delta H_C}{\rho c_p (T_O - T_F)} \cdot \frac{D_F^*}{\left|U_F^*\right|} \tag{9}$$

$$\frac{\partial Y_i}{\partial t} + u\frac{\partial Y_i}{\partial x} + v\frac{\partial Y_i}{\partial y} = \frac{1}{Pe\,Le_i}\left(\frac{\partial^2 Y_i}{\partial x^2} + \frac{\partial^2 Y_i}{\partial y^2}\right) - \frac{D_F^*}{\left|U_F^*\right|}\frac{\dot{\omega}_i^*}{\rho} \tag{10}$$

where α is the thermal diffusivity, ΔH_C is the heat release rate and $Y_i^*, \dot{\omega}_i^*$ are, respectively, the mass fraction in the mixture and consumption rate of the "i" specie. The mass diffusivity coefficients are considered equal for each species ($D_{ij} = D_{ji} = D$). The Simple Chemical Reaction System (SRCS) hypothesis is employed and the Shvab-Zel'dovich potential conservation equation can be obtained by following the assumption:

$$1\ \text{kg of Fuel} + s\ \text{kg of Oxidizer} \longrightarrow (1+s)\ \text{kg of Products} \tag{11}$$

For stoichiometric coefficients, n_F, n_O, and molecular weights of fuel and oxidizer, W_F, W_O, the mass-weighted stoichiometric coefficient ratio (s) can be written as:

$$s = \frac{n_O . W_O}{n_F . W_F} \tag{12}$$

As consequence, the species consumption rates can be written as:

$$\dot{\omega}_F^* = \frac{\dot{\omega}_O^*}{s} \tag{13}$$

Assuming $Le_F = Le_O = 1,$ and manipulating the species equations - Eqs. (10) - the first Shvab-Zel'dovich potential and the correspondent conservation equation can be established as follows by:

$$\phi_{FO} = Y_F - \frac{Y_O}{s} \tag{14}$$

$$\frac{\partial \phi_{FO}}{\partial t} + u\frac{\partial \phi_{FO}}{\partial x} + v\frac{\partial \phi_{FO}}{\partial y} = \frac{1}{Pe}\left(\frac{\partial^2 \phi_{FO}}{\partial x^2} + \frac{\partial^2 \phi_{FO}}{\partial y^2}\right) \tag{15}$$

In a similar way, the other two potentials and the dimensionless heat release rate (Q) can be expressed as:

$$\phi_{TF} = Q.Y_F + \theta \quad ; \quad \phi_{TO} = \frac{Q.Y_O}{s} + \theta \quad \text{and} \quad Q = \frac{\Delta H_C}{c_p(T_O - T_F)} \tag{16.a-c}$$

resulting in a linear relation between the Shvab-Zel'dovich potentials:

$$\phi_{TO} = \phi_{TF} - Q.\phi_{FO} \tag{17}$$

Of all fuels of commonly studied, hydrogen is unique for its high diffusivity. The Lewis number of hydrogen is approximately 0.3. Methane, in contrast, has a Lewis number close to unity, which agrees with the unitary Lewis number hypothesis. Due to the Lewis number difference, hydrogen flames are subject to strong cellular instabilities that lead to structures and phenomena not associated with hydrocarbon fuels. The Prandtl number was chosen *0.7*, resulting in a Reynolds-dependent Peclet number.

For inert and isolated walls, the species mass fractions and temperature boundary conditions on the walls satisfy a zero-flux condition as depicted in Fig.2.

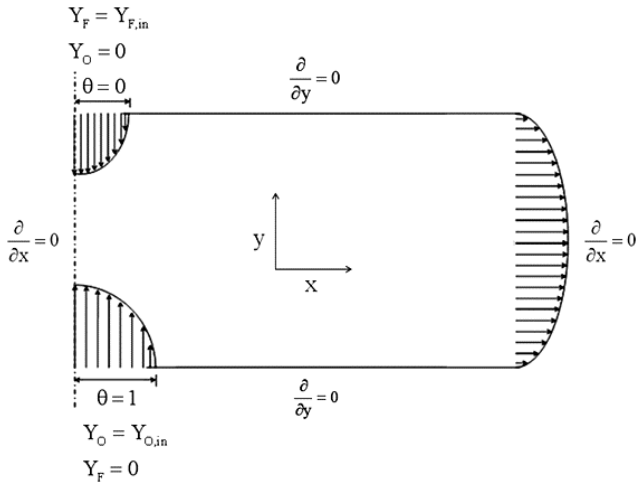

Figure 2. Scketch of the mass fractions and temperature boundary conditions.

The subscripts "in" and "St" means, respectively, nozzle and stoichiometric conditions. The initial condition corresponds to stagnated fluid (atmospheric air) at 300 K.

5. Numerical Procedure

The Finite-Difference Method is employed on the resulting conservation equations, which are discretized using the BTCS (Backward in Time Forward in Space) scheme. An iterative numerical technique, based on the algorithm of the Gauss-Seidel with successive under-relaxation and local error control is applied to solve the resulting algebraic linear systems.

5.1. Mesh Analysis

Initially a mesh analysis is conducted in order to select analyze the precision and the computational requirements of the developed codes Meshes with *21x21*, *41x41* and *81x81* points were investigated. The following results were computed using the *41 x 41* mesh points. Figure 3 shows the vorticity and the stream function results at $x = 1.5$, with for $Re = 100$, $R_V = 4$, $R_B = 1$, $R_{DL} = 1$ and $R_H = 4$.

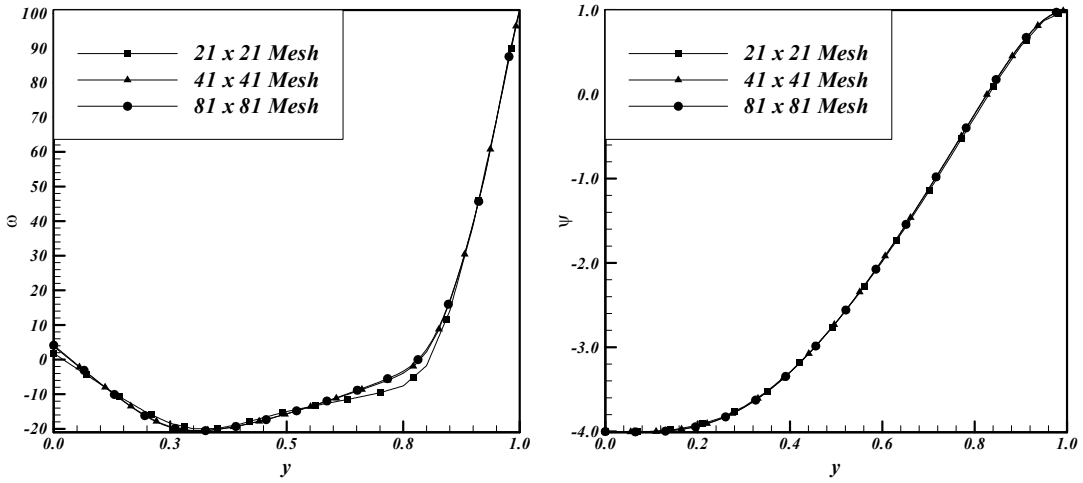

(a) (b)

Figure 3. Vorticity (a) and Stream function (b) plots at x = 1.5.

The stream function results show convergence within the precision of the graphics and the deviations observed indicate the usage of the *41 x 41* mesh. For the vorticity, the maximum relative error was *8.9%* at $y = 0,724$ between the refined meshes. Between the less refined meshes the maximum deviation was *47.8%* at $y = 0.748$. For the stream function results, the maximum relative error between the *21x21* and the *41x41*meshes was 3.18 % at $y = 0.975$. Between the two more refined ones the stream function deviation was *0.78 %*, at $y = 0.978$. Based on these results, the 41 x 41 point mesh was adopted in the present work.

5.2. Domain Truncation Analysis

Tests were also performed in order to define an appropriate position for the outflow boundary where the zero flux condition is applied. Test results available in the literature (Frouzakis *et al* ,2002) indicate that good agreement for truncation positions are expected for $R_H = 6$. Vorticity and stream function results are depicted in Fig. 4, and the Fig. 5 shows the results for horizontal velocity component and the first Shvab-Zel'dovich potential at $x = 2.5$, for three different domain truncation positions. The results shown in Figs.4 and 5 were obtained for $Re = 232$, $R_V = 1$, $R_B = 1$, $R_{DL} = 0.5$.

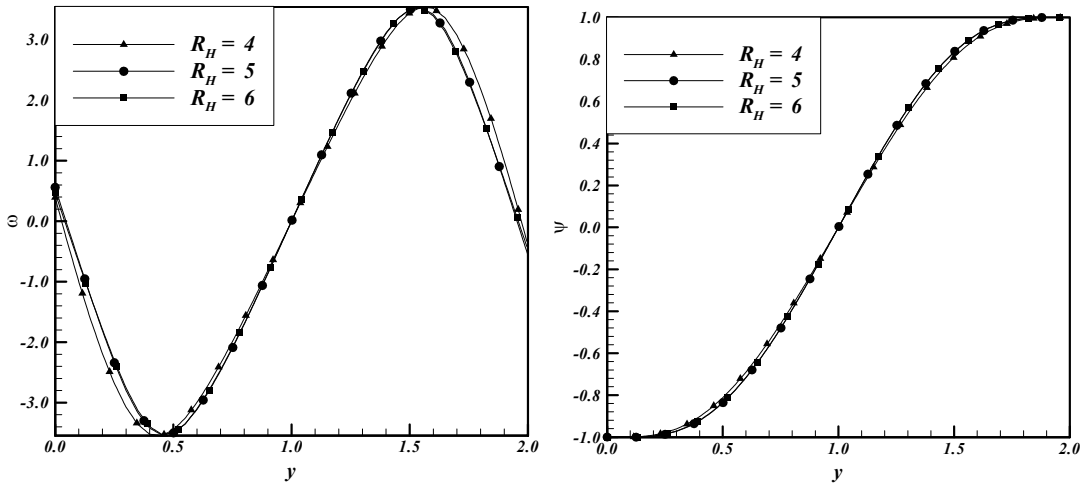

(a) (b)

Figure 4. Vorticity (a) and Stream function (b) plots at x = 2.5.

For the vorticity, the maximum relative error between was *1.23%* at $y = 0.35$ when results obtained for $R_H = 5$ and $R_H = 6$ are compared. Between the results for $R_H = 4$ and $R_H = 5$ the vorticity difference was *15.7%* at $y = 1.78$. For the stream function, the maximum relative error of *0.15%* was observed when results for $R_H = 5$ *and* $R_H = 6$ are compared. Between the results for $R_H = 4$ and $R_H = 5$, the maximum difference on the stream function was *3.8%* at $y = 1.39$.

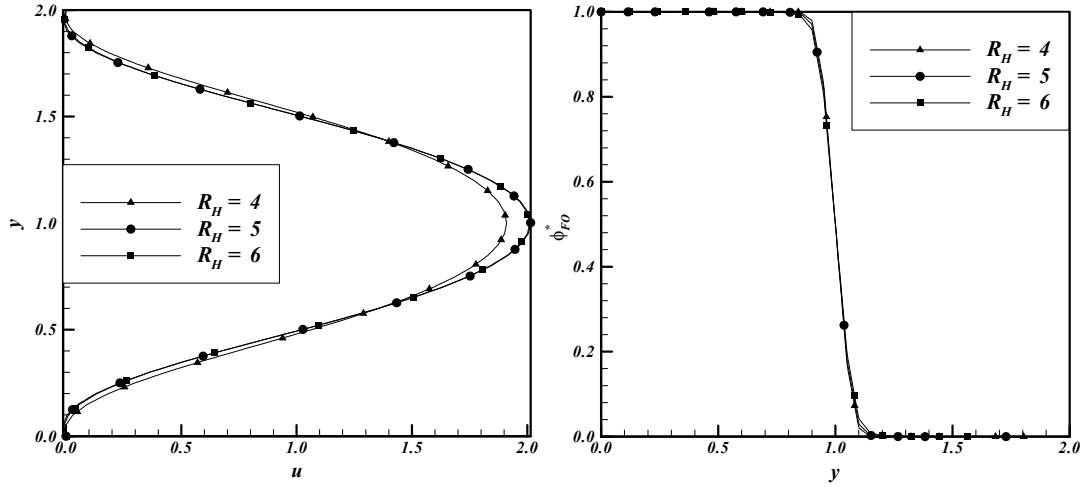

(a) (b)

Figure 5. Horizontal velocity component (a) and first Shvab-Zel'dovich potential (b) at x = 2.5.

For the horizontal velocity component, the maximum relative error between $R_H = 5$ and $R_H = 6$ was smaller than *0.15%,* while between $R_H = 4$ and $R_H = 5$ was *5.16%* at $y = 1$. The first Shvab-Zel'dovich potential presented maximum absolute errors of *0.012* between $R_H = 4$ and $R_H = 5$ and *0.0091* between to $R_H = 5$ and $R_H = 6$, at $y = 1.1$.

6. Results

6.1. Methane-Air, $Re = 20$, $R_V = 1$.

Results obtained for a methane-air flame on a *0.5 cm x 3.0 cm* domain, considering equal inflow species velocities ($R_V = 1$) and $Re = 20$ are initially discussed. The thermo-physical properties are chosen as $\Delta H_C = 802$ *kJ/mol* (Kuo, 1986); $c_p = 30$ *J/mol.K*; $T_O = 400$ *K*; $T_F = 300$ *K*; $Y_{O,in} = 0.233$; $Y_{F,in} = 1$ and $\phi^*_{\mathrm{FO,St}} = 0.05518$. The specific heat at constant pressure was considered constant at the average value between the air and the fuel at the nozzles temperatures (Fachini, 2004). The hydrodynamic and geometric parameters are set to $R_{DL} = 0.5$, $R_B = 1$, $R_H = 6$.

Results in Fig. 6.b shows the temperature distribution and the stoichiometric line and the temperature, oxidizer and fuel mass fraction profiles, within the nozzle region ($x = 0.8$), The calculated dimensionless adiabatic flame temperature was 15,7 (1869 K).

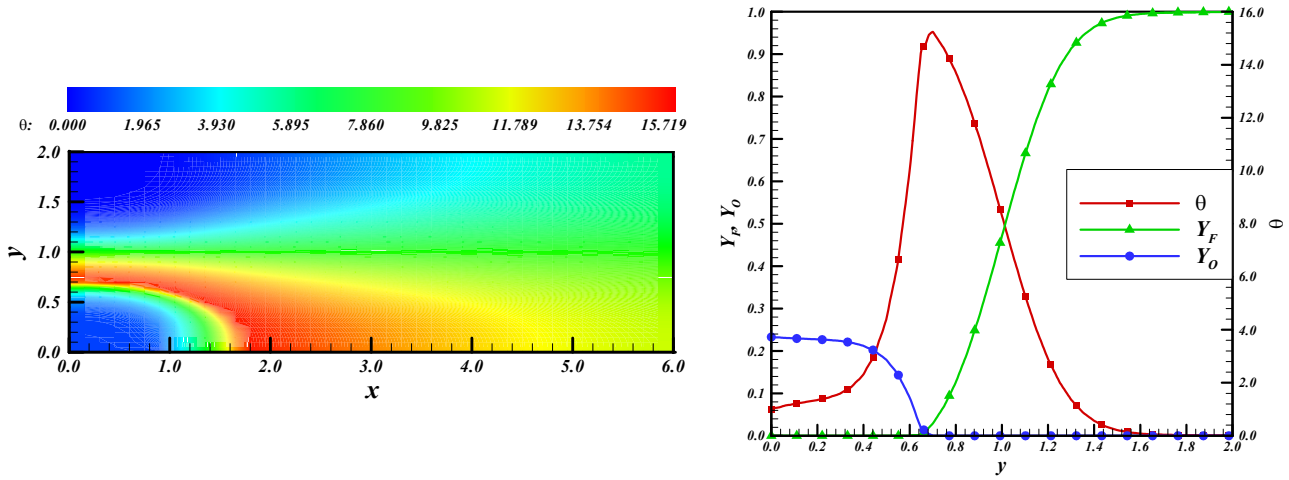

(a) (b)

Figure 6. (a) Temperature field and stoichiometric line and (b) temperature, oxidizer and fuel profiles, at x = 0.8

An under-ventilated flame can be observed in Fig.6.a. The low Reynolds number imposes the flame to bend towards the oxidizer nozzle. It is important to remember that the flow stagnation plane is located at $y = 1$, due to the $R_V = 1$ choice. It is expected that increasing R_V the recirculation zone close to the oxidizer nozzle will become larger too. Besides, the stagnation plane will move towards the fuel nozzle, reorienting the flame's shape and position to the new flow condition.

6.2. Methane-Air, $Re = 20$, $R_V = 2$

Increasing the oxidizer inflow velocity by setting $R_V = 2$, the stagnation plane is displaced upwards. Figure 7.a shows the temperature distribution field, the stoichiometric line and the velocities profiles at the nozzles and along the cross-sections, allowing the visualization of the developing parabolic profiles towards the outflow region. Stream function contours are also shown in Fig.7.

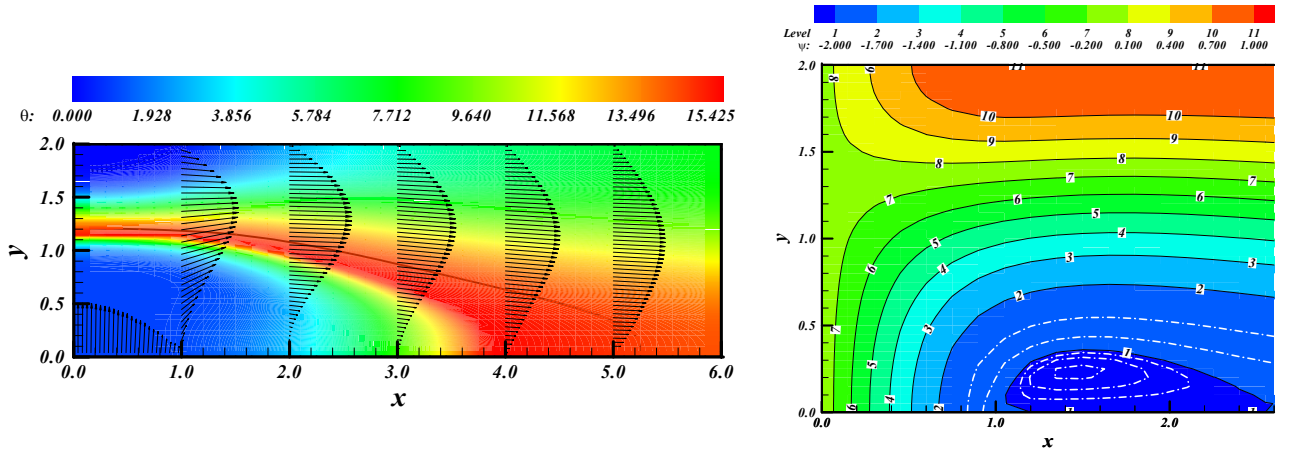

(a) (b)

Figure 7. (a) Temperature field, stoichiometric line and velocities profiles and (b) stream function contours.

From the stream function contours depicted in Fig. 7.b, it is possible to visualize the new stagnation plane location and the presence of a recirculation zone close to bottom wall, between $x = 1.2$ and $x = 2.2$. Stream function isolevels within the recirculation zone are represented in white dashed lines. A detailed view of the recirculation zone near the oxidizer wall is shown in Fig.8.

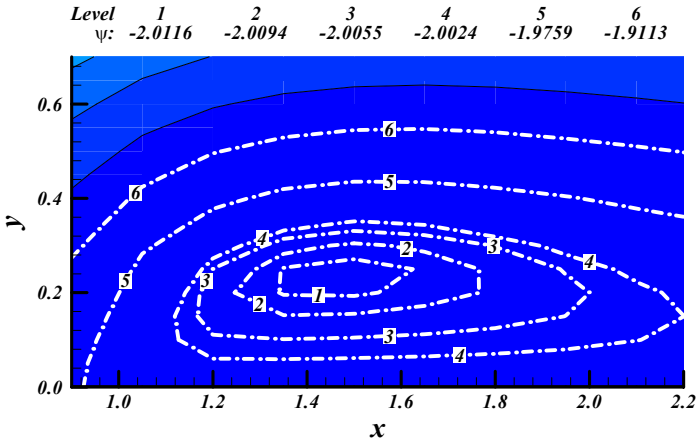

Figure 8. Recirculation zone (closer view).

6. Conclusions

In the present work a procedure for the analysis of the structure of a confined methane-air flame, subject to a parametric analysis where effects of the inflow velocities ratio and the horizontal truncation domain position is introduced. Due to the presence of the two solid boundaries, a significant recirculation zone develops, especially at high inlet velocities. Although recirculation zones are known to alter the stability of flames, our 2-D simulation results agree well with experimental observations obtained without confinement (Pellet et al, 1998).

A discussion on the parameters for the numerical simulation is also presented. The results became independent of the truncation distance for $R_H = 6$. Future work will focus on the study the effects of Lewis and Grashoff numbers, fuel composition and inlet temperature to determine accurately (and more efficiently) some critical parameters, using the Shvab-Zel'dovich results as initial condition for a finite-chemistry model.

8. References

Anderson, D.A., *et al*., 1984, "Computational Fluid Mechanics and Heat Transfer", New York: Hemisphere Publishing Corporation.

Chaniotis, A. K., Frouzakis, C. E., Lee, J. C., *et al*, 2003, "Remeshed smoothed particle hydrodynamics for the simulation of laminar chemically reactive flows", Journal of Computational Physics, Vol. 191, No.1, pp. 1-17.

Daou, J. and Liñán, A., 1999, "Ignition and extinction fronts in counterflowing premixed reactive gases", Combustion and Flame Vol. 118, pp. 479-488.

Douglas, C. C., Ern, A., and Smooke, M. D., 1996, "Numerical Simulation of Laminar Diffusion Flames", SIAM News, 27/9, pp. 1, 12-13, 17. To appear in revised form in Applications on Advanced Architecture Computers, G. Astfalk (ed.), SIAM Books, Philadelphia.

Fachini, F. F., 2001, "N-Fuels Diffusion Flame: Counterflow Configuration", In: Proceedings of XVI Congresso Brasileiro de Engenharia Mecânica, CD ROM, Uberlândia.

Fachini, F. F., 2004, Multicomponent Fuel Diffusion Flames: A General Shvab-Zel'dovich Formulation, "under consideration for publication", Vol.

Frouzakis, C. E., Lee, J. C., Tomboulides, D., *et al*, 2002, "From diffusion to premixed flames in an H_2-Air opposed-jet burner: the role of edge flames", Combustion and Flame, Vol. 130, pp.171-184.

Kuo, K. K., 1986, "Principles of Combustion", USA, Wiley-Interscience.

Pellett, G. L., Isaac, K. M., Humphreys, W. M., *et al*, 1998, "Velocity and Thermal Structure, and Strain- Induced Extinction of 14 to 100% Hydrogen-Air Counterflow Diffusion Flames", Combustion and Flame, Vol. 112, No. 4, pp. 575-592.

Santoro, V.S., Kyritsis, D.C., Gomez, A., 1999, "Extinction Behavior of either Gaseous or Spray Counterflow Diffusion Flames Interacting with a Laminar Toroidal Vortex", 17th International Colloquium on the Dynamics of Explosions and Reactive Systems, Heidelberg, Germany.

Tomboulides, A.G., Lee, J.C., Orszag, S.A., 1997, "Numerical Simulation of Low Mach Number Reactive Flows", Journal of Scientific Computing, Vol. 12, No. 2, pp. 139-167.

Tsuji, H., 1982, "Counterflow Diffusion Flames", Progress Energy Combustion Science, Vol.8, pp. 93-119.

Williams, B. A., 2001, "Sensitivity of calculated extinction strain rate to molecular transport formation in non-premixed counterflow flames", Combustion and Flame, Vol. 124, pp. 330–333.